Axisymetric eigenmodes and soft iron in the von-Kármán-Sodium dynamo

A. Giesecke, F. Stefani & G. Gerbeth
Helmholtz-Zentrum Dresden-Rossendorf

in collaboration with
C. Nore, F. Luddens & W. Herreman (LIMSI, Orsay),
J. Léorat (Observatoire Paris-Meudon),
J.-L. Guermond (Texas A&M University)

EGU General Assembly 2012,
Vienna, April 23 - 27, 2012

We are grateful for support by the DFG collaborate research center SFB–609.

Motivation: Von-Kármán-Sodium (VKS) dynamo

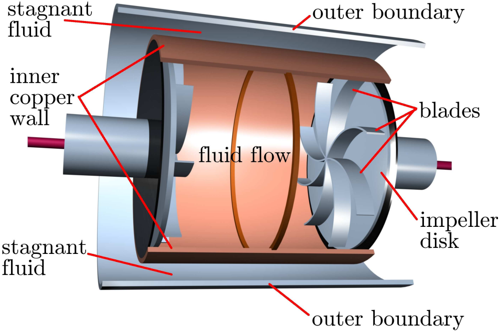

from Monchaux et al., PRL, 2007

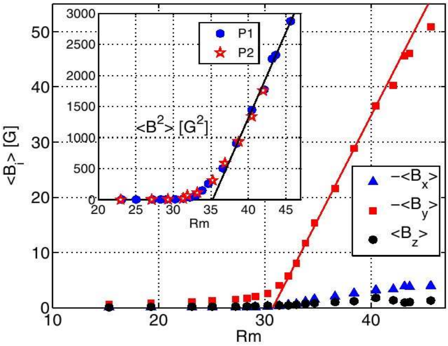

- flow of liquid sodium driven by two counterrotating impellers
- mean flow structure: two poloidal cells, two toroidal cells ($S_2 T_2$)
- bended blades for optimization of poloidal to toroidal velocity ratio

- axisymmetric dynamo action but only with soft iron impellers with permeability $\mu_r \approx 65$
- manifold field characteristics: (quasi-)stationary, bursts, oscillations, reversals, hemispherical

Non-uniform conductivity/permeability

$$\frac{\partial \mathbf{B}}{\partial t} = \nabla \times \left[(\mathbf{u} \times \mathbf{B}) + \frac{1}{\mu_0 \mu_r \sigma} (\nabla \ln \mu_r \times \mathbf{B}) - \frac{1}{\mu_0 \mu_r \sigma} (\nabla \times \mathbf{B}) \right]$$

- non-uniform conductivity/permeability provides potential "support" of dynamo action by coupling of B^{tor} and B^{pol}

$\Rightarrow$ Busse/Wicht: periodic conductivity modulation & uniform flow

- additional term in the induction equation that acts like a velocity $\mathbf{V}^{\mu} = \frac{\nabla \ln \mu_r}{\mu_0 \sigma \mu_r}$ with $\nabla \cdot \mathbf{V}^{\mu} \neq 0$

$\Rightarrow$ **paramagnetic pumping:** i.e. suction of magnetic field into region with larger μ_r

Internal jump conditions for B and E

$$\mathbf{n} \cdot (\mathbf{B}_1 - \mathbf{B}_2) = 0 \qquad \mathbf{n} \times \left(\frac{\mathbf{B}_1}{\mu_{r,1}} - \frac{\mathbf{B}_2}{\mu_{r,1}}\right) = 0 \quad \text{for permeability jump}$$

$$\mathbf{n} \cdot (\mathbf{j}_1 - \mathbf{j}_2) = 0 \qquad \mathbf{n} \times (\mathbf{E}_1 - \mathbf{E}_2) = 0 \quad \text{for conductivity jump}$$

Kinematic solution of the induction equation

numerical solutions of induction equation with non-uniform μ_r & σ

$$\frac{\partial}{\partial t}\mathbf{B} = \nabla \times \left(\mathbf{u} \times \mathbf{B} - \frac{1}{\mu\sigma(\mathbf{r})} \nabla \times \frac{\mathbf{B}}{\mu_\mathrm{r}(\mathbf{r})} \right)$$

- prescribed velocity field $\mathbf{u}(\mathbf{r})$
- no backreaction on the flow
- here: spatial variations of μ_r

- kinematic approach: $\mathbf{B} \sim \mathbf{B}_0 e^{\gamma t} \Rightarrow \gamma \mathbf{B} = \mathcal{M}\mathbf{B}$
  $\Rightarrow$ compute growth rates (eigenvalues) and dynamo eigenmodes
  $\Rightarrow$ dominant field geometry (azimuthal mode, equatorial symmetry)

Numerical approach

- turbulence unimportant $\Rightarrow$ induction caused by mean flow alone
- numerical simulations with 2 distinct schemes
  (1) spectral/finite element approximation (SFEmANS, Guermond et al.)
  (2) hybrid finite volume/boundary element method (timestepping)

$\Rightarrow$ insulating boundary conditions & arbitarly spatial distributions for σ, μ_r (axisymmetric for spectral scheme)

Prescribed velocity field & numerical approach

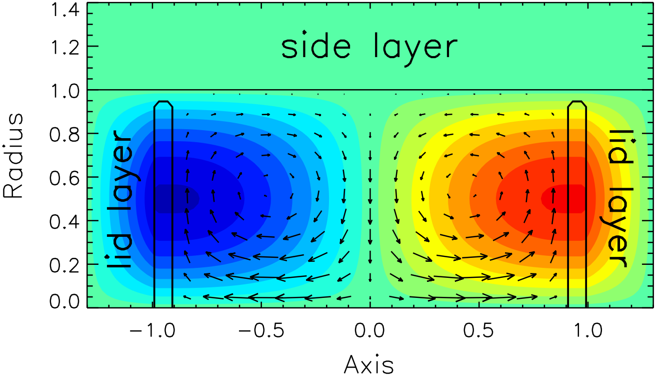

- MND bulk flow: $\mathbf{v} = \nabla \times \mathbf{A}$ with $\mathbf{A} \propto (f_1(r)\sin(\pi z/2H), 0, f_2(r)\sin(\pi z/H))$
  $\Rightarrow$ laminar flow with *S2T2* topology: 2 poloidal & 2 toroidal eddies
- side layer with stagnant fluid & lid layers behind impellers
- disks: axisymmetric distributon with large permeability $\mu_{\mathrm{r}} = 1 \cdots 100$
- no internal boundary conditions between disks and fluid flow

Growth rates for the axisymmetric mode ($m0$)

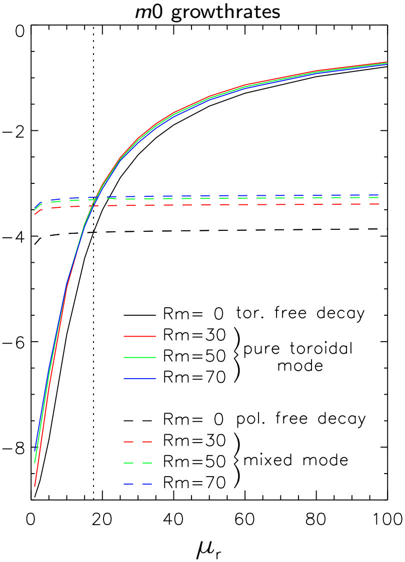

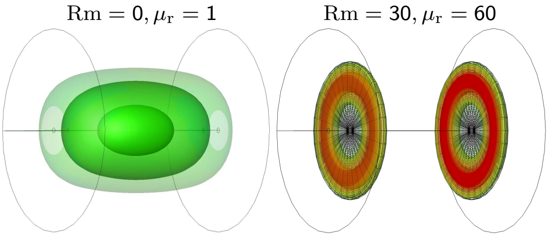

- significant shift towards dynamo threshold (but only B_φ): *purely toroidal* mode becomes dominant for $\mu_\mathrm{r} \gtrsim 17$
- *mixed mode* hardly affected by μ_r
- flow magnitude (Rm) and BC unimportant for $\mu_\mathrm{r} \gg 1$
- Cowling also valid for $\mu_\mathrm{r} = \mu_\mathrm{r}(\mathbf{r}, t)$ $\Rightarrow$ no $m0$ dynamo action possible

Comparison of $m0$- and $m1$-mode

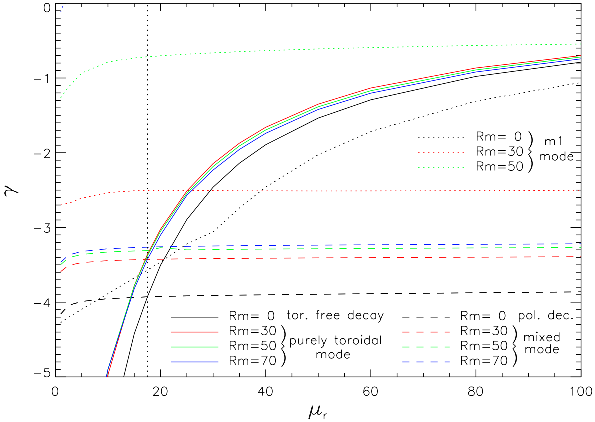

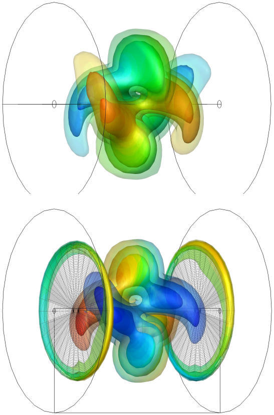

- $\mathrm{Rm} \approx 30...40 \Rightarrow$ axisymmetric B_φ dominates for $\mu_\mathrm{r} \gg 1$
- fast decay of poloidal $m0$ mode (even faster than $m1$ mode)
- sufficient large $\mathrm{Rm} \Rightarrow$ "equatorial" ($m1$) dynamo ($\mathrm{Rm}^\mathrm{c} \approx 63$)

Coupling of poloidal and toroidal components

- consider axisymmetric part of induction equation $(b_r^0, b_z^0, b_\varphi^0)$

$$\frac{\partial b_r^0}{\partial t} = -\frac{\partial}{\partial z}(u_z b_r^0 - u_r b_z^0) - \eta \left[-\frac{\partial}{\partial z} \left(\frac{\partial}{\partial z} \frac{b_r^0}{\mu_\mathrm{r}} - \frac{\partial}{\partial r} \frac{b_z^0}{\mu_\mathrm{r}} \right) \right]$$

$$\frac{\partial b_\varphi^0}{\partial t} = \frac{\partial}{\partial z}(u_\varphi b_z^0 - u_z b_\varphi^0) - \frac{\partial}{\partial r}(u_r b_\varphi^0 - u_\varphi b_r^0) - \eta \left[-\frac{\partial^2}{\partial z^2} \frac{b_\varphi^0}{\mu_\mathrm{r}} - \frac{\partial}{\partial r} \left(\frac{1}{r} \frac{\partial}{\partial r} \left(r \frac{b_\varphi^0}{\mu_\mathrm{r}} \right) \right) \right]$$

$$\frac{\partial b_z^0}{\partial t} = \frac{1}{r} \frac{\partial}{\partial r} \left[r \left(u_z b_r^0 - u_r b_z^0 \right) \right] - \eta \frac{1}{r} \frac{\partial}{\partial r} \left[r \left(\frac{\partial}{\partial z} \frac{b_r^0}{\mu_\mathrm{r}} - \frac{\partial}{\partial r} \frac{b_z^0}{\mu_\mathrm{r}} \right) \right]$$

- $b_r^0, b_z^0 = 0$ & $b_\varphi^0 \neq 0$ is a possible solution $\Rightarrow$ purely toroidal mode
- $b_r^0, b_z^0 \neq 0 \Rightarrow$ shearing by $u_\varphi \Rightarrow b_\varphi^0 \neq 0 \Rightarrow$ mixed mode
- growth rate of mixed mode is fixed by its poloidal components! $\Rightarrow b_\varphi^0$ "follows" b_r^0, b_z^0 but there is no way to transfer magnetic field from toroidal to poloidal component $\Rightarrow b_r^0, b_z^0$ cannot "follow" b_φ^0

Selective enhancement of axisymmetric B_φ

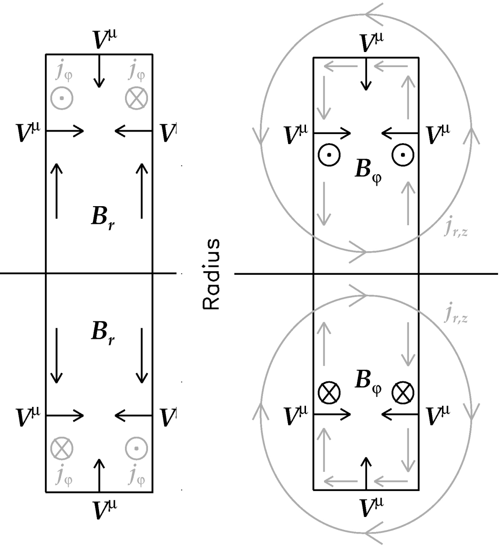

- at the fluid-disk interface paramagentic pumping causes a localized electromotive force:
  $\mathcal{E}^\mu = \mathbf{V}^\mu \times \mathbf{B} = \frac{1}{\mu_0 \sigma \mu_r} \frac{\nabla \mu_r}{\mu_r} \times \mathbf{B}$
  which drives an electric current

Selective enhancement of axisymmetric B_φ

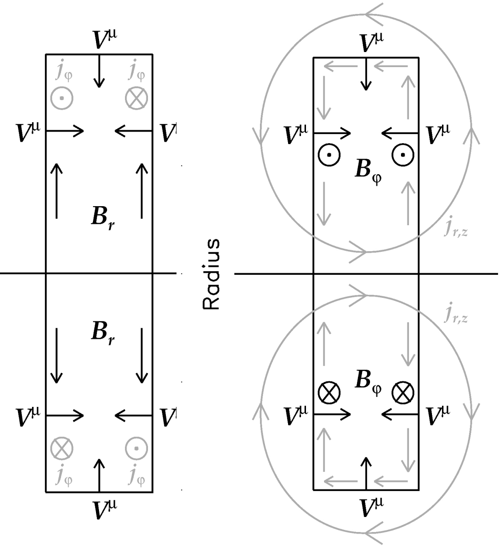

- at the fluid-disk interface paramagentic pumping causes a localized electromotive force: $\mathcal{E}^\mu = \mathbf{V}^\mu \times \mathbf{B} = \frac{1}{\mu_0 \sigma \mu_r} \frac{\nabla \mu_r}{\mu_r} \times \mathbf{B}$ which drives an electric current
- thin disks $\Rightarrow \mathbf{V}^\mu \propto \frac{\partial \mu_r}{\partial z} \mathbf{e}_z$

  $\Rightarrow$ no interaction with $B_z \mathbf{e}_z$

Selective enhancement of axisymmetric B_φ

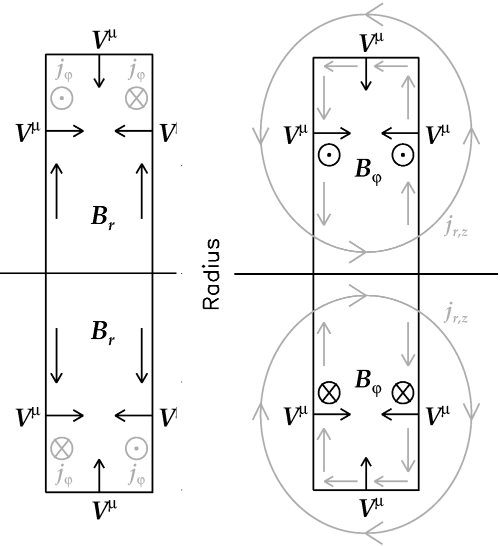

- at the fluid-disk interface paramagentic pumping causes a localized electromotive force: $\mathcal{E}^\mu = \mathbf{V}^\mu \times \mathbf{B} = \frac{1}{\mu_0 \sigma \mu_r} \frac{\nabla \mu_r}{\mu_r} \times \mathbf{B}$ which drives an electric current
- thin disks $\Rightarrow \mathbf{V}^\mu \propto \frac{\partial \mu_r}{\partial z} \mathbf{e}_z$ $\Rightarrow$ no interaction with $B_z \mathbf{e}_z$
- interaction of $B_r \mathbf{e}_r$ and $\mathbf{V}^\mu$ $\Rightarrow$ azimuthal currents with opposite sign at front/back side

Selective enhancement of axisymmetric B_φ

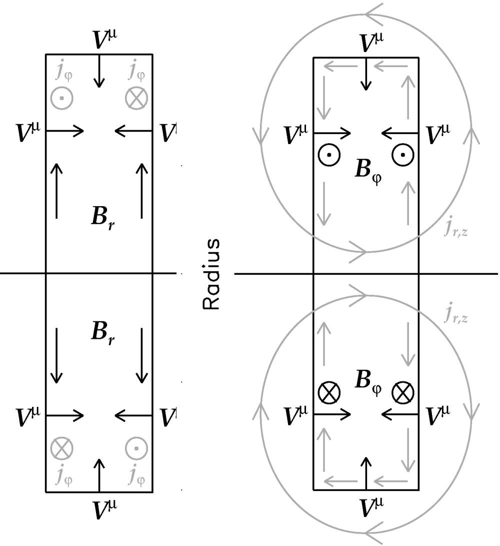

- at the fluid-disk interface paramagentic pumping causes a localized electromotive force:
  $\mathcal{E}^\mu = \mathbf{V}^\mu \times \mathbf{B} = \frac{1}{\mu_0 \sigma \mu_\mathrm{r}} \frac{\nabla \mu_\mathrm{r}}{\mu_\mathrm{r}} \times \mathbf{B}$
  which drives an electric current
- thin disks $\Rightarrow \mathbf{V}^\mu \propto \frac{\partial \mu_\mathrm{r}}{\partial z} \mathbf{e}_z$
  $\Rightarrow$ no interaction with $B_z \mathbf{e}_z$
- interaction of $B_r \mathbf{e}_r$ and $\mathbf{V}^\mu$
  $\Rightarrow$ azimuthal currents with opposite sign at front/back side
- interaction of $B_\varphi \mathbf{e}_\varphi$ and $\mathbf{V}^\mu$ gives rise for an axisymmetric poloidal current $\mathbf{j}^\mathrm{p} = j_r \mathbf{e}_r + j_z \mathbf{e}_z$

$\Rightarrow$ sustainment/amplification of B_φ

(1) localized high permeability domain within conducting fluid flow is responsible for paramagnetic pumping

selective enhancement of B_φ and domination of an axisymmetric purely toroidal mode that is hardly affected by the flow

(2) a second axisymmetric mode consisting of a poloidal and a toroidal component (mixed mode) is hardly affected by μ_r and lies below the purely toroidal mode or the m1-mode

(3) the purely toroidal mode can be obtained only by explicitly considering the internal permeability distribution and the jump conditions at the fluid-disk interface

the purely toroidal mode may play an important role for axisymmetric dynamo action but in our simple axisymmetric set-up no possibility for a closure of the dynamo cycle is provided (**Cowling's theorem** is valid also for time and space dependent σ & μ_r (Hide & Palmer))

Problems & Outlook

- non-axisymmetric μ_{r} couples a poloidal mode to the (previously) purely toroidal mode $\Rightarrow$ **role of blades?**
  $\Rightarrow$ but coupling also from azimuthal σ variation
- dominant purely toroidal mode does not exists for high/low conducting disks because there is no enhancement mechanism
- growing axisymmetric solutions can be obtained applying mean field effects that parametrize induction of small scale turbulent flow (α-effect, $\mathbf{\Omega} \times \mathbf{j}$-effect), e.g. a growing *m*0-mode is possible for very small α–effect (Giesecke et al. PRL 104, 2010) but existence and pattern of α in the experiment remains unknown

Simplified model for the toroidal $m0$-mode

purely toroidal mode is mostly localized inside disks and impact of flow remains negligible $\Rightarrow$ idealized disk-fluid model with free decay

- disk with radius $R = 1$, permeability $\mu_\mathrm{r} \gg 1$ and thickness d within infinite cylindrical fluid region with $\mu_\mathrm{r} = 1$

$$
\begin{aligned}
\mu_\mathrm{r}\gamma B_\varphi &= \left(\frac{\partial^2}{\partial r^2} + \frac{1}{r}\frac{\partial}{\partial r} + \frac{\partial^2}{\partial z^2} - \frac{1}{r^2}\right)B_\varphi, \quad r < 1 \quad |z| < d/2 \\
\gamma B_\varphi &= \left(\frac{\partial^2}{\partial r^2} + \frac{1}{r}\frac{\partial}{\partial r} + \frac{\partial^2}{\partial z^2} - \frac{1}{r^2}\right)B_\varphi, \quad r < 1 \quad |z| > d/2
\end{aligned}
$$

BC: $B_\varphi = 0$ at $r = 1$ and symmetry considerations suggest:

$$
\begin{aligned}
B_\varphi &= A_1 J_1(kr)\cos l_1 z, \quad r < 1, \quad |z| < d/2, \quad l_1 = \sqrt{-\gamma\mu_\mathrm{r} - k^2} \\
B_\varphi &= A_2 J_1(kr) e^{-l_2 z}, \quad r < 1, \quad |z| > d/2 \quad l_2 = \sqrt{k^2 + \gamma}
\end{aligned}
$$

J_1: Bessel function of 1st kind, $k \approx 3.8317$ to fulfill $B_\varphi = 0$ at $r = 1$

$\Rightarrow$ implicit non-linear equation for γ as function of d and μ_r:

$$
l_2 \cos\left(\frac{l_1 d}{2}\right) - l_1 \sin\left(\frac{l_1 d}{2}\right) = 0
$$

Comparison with numerical solutions

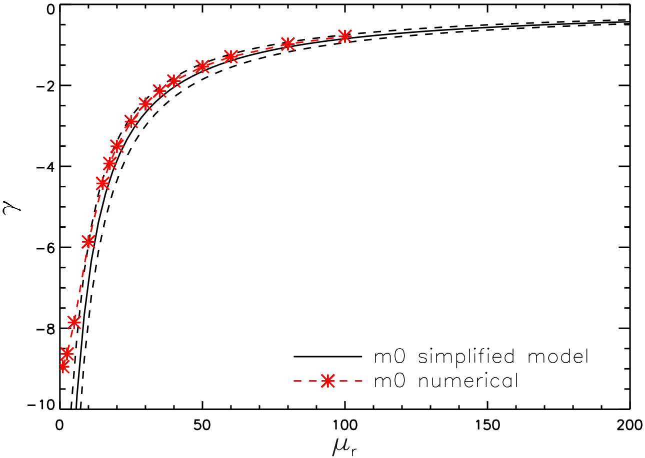

- $\gamma(\mu_r) \sim \mu_r^{-1}$ in the limit $\mu_r \to \infty$
- good agreement between simple analytical model and numerical simulations

$\Rightarrow$ although the dominant purely toroidal mode is localized to a very small volume its decay time determines the overall decay of the axisymmetric azimuthal magnetic field.

EMF & electric current

Electromotive force: $\mathcal{E} \propto \frac{\nabla \mu_{\rm r}}{\mu_{\rm r}} \times \mathbf{B}$

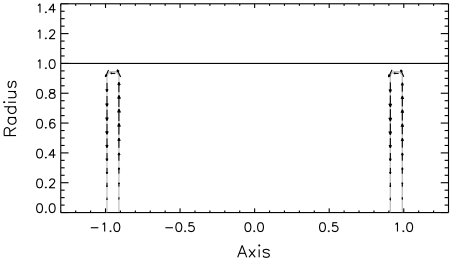

poloidal current: $\mathbf{j}^{\rm p} \propto (\nabla \times \mathbf{H})_{r,z}$

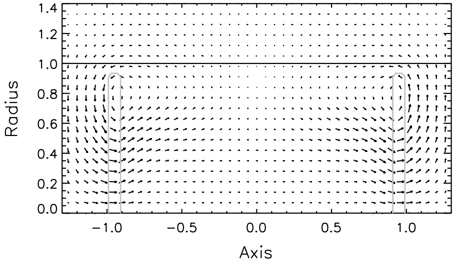

- loacalized EMF (left) drives poloidal axisymmetric current concentrated around the impellers (right)
- $\mathbf{j}^{\rm p}$ is source for the enhancement of azimuthal axisymmetric field mode but does not provide a dynamo source
- azimuthal current remains negligible

Growth rates for $m1$ mode

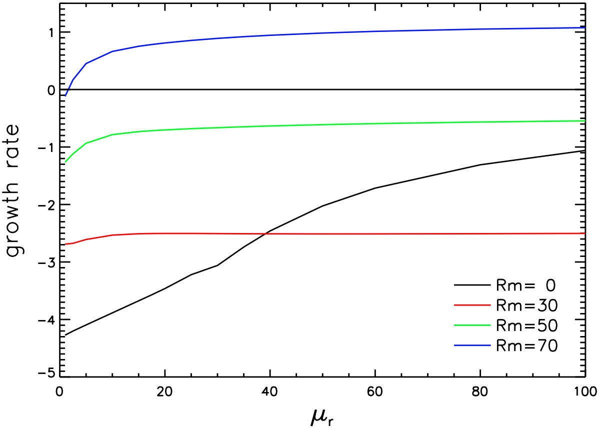

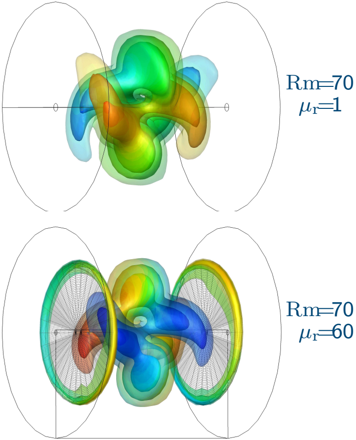

- growth rates increases with increasing μ_r (saturation for $\mu_r \gg 1$)
  $\Rightarrow$ reduction from $\mathrm{Rm}^c = 76$ for $\mu_r = 1$ to $\mathrm{Rm}^c = 55$ for $\mu_r = 100$
- distinct behavior for free decay $(\mathrm{Rm} = 0)$ and $\mathrm{Rm} > 0$

HZDR HELMHOLTZ ZENTRUM DRESDEN ROSSENDORF

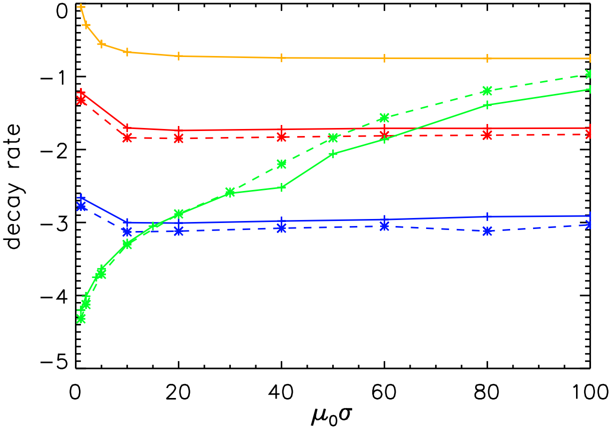

- increasing $\mu_0\sigma \Rightarrow$ increase of $\mathrm{Rm}^{\mathrm{crit}} \rightarrow \gtrsim 80$

Decay rates

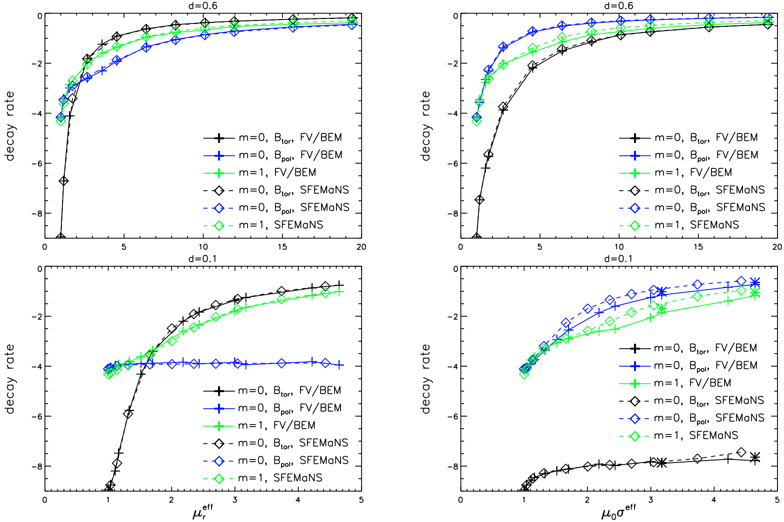

thick disk $d = 0.6$

thinn disk $d = 0.1$

poloidal field supressed with increasing μ_{r}

toroidal field supressed with increasing $\mu_0\sigma$

External boundary conditions

Vacuum BC | Vanishing tangential field BC

$\mu_r = 1$

$\mu_r = 100$

$\mu_0\sigma = 100$

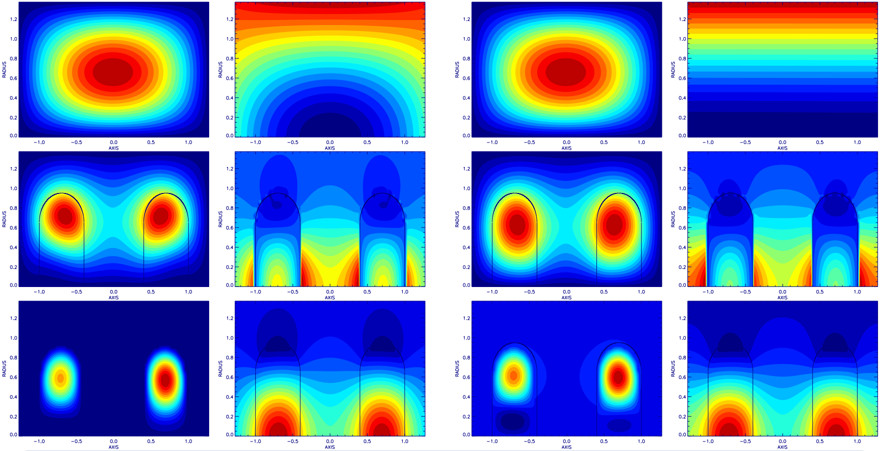

- Internal jump conditions are more important than external BC

$$\mathbf{n}\cdot(\mathbf{B_1}-\mathbf{B_2}) = 0 \qquad \mathbf{n}\times(\mathbf{B_1}/\mu_{r,1}-\mathbf{B_2}/\mu_{r,1}) = 0$$

$$\mathbf{n}\cdot(\mathbf{j_1}-\mathbf{j_2}) = 0 \qquad \mathbf{n}\times(\mathbf{E_1}-\mathbf{E_2}) = 0$$

External BC

HZDR HELMHOLTZ ZENTRUM DRESDEN ROSSENDORF

Decay times: $\tau = (\gamma)^{-1}$

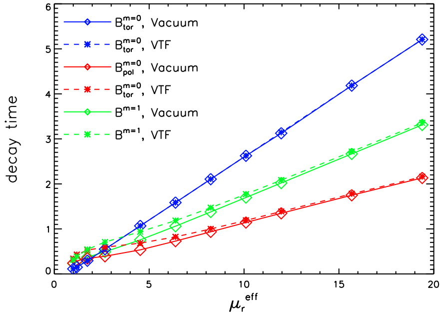

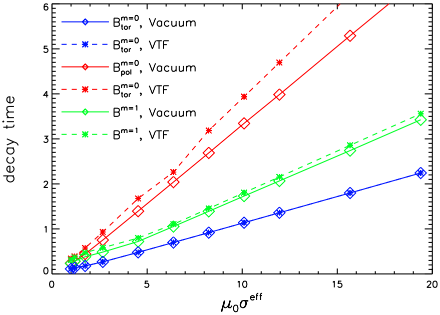

- vanishing tangential fields or pseudo vacuum resemble setup with infinite permeability in the exteriour
- nearly no influence in comparison with insulating boundary conditions

Ohmic decay

B_r

B_φ

B_z

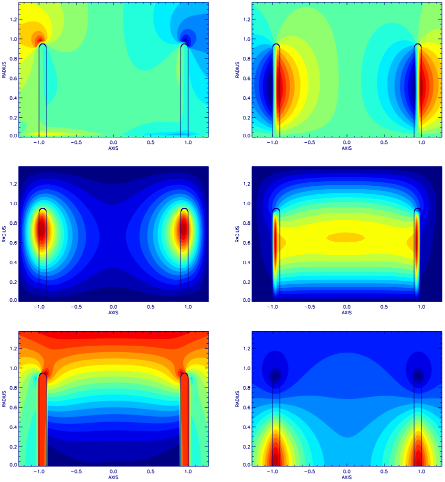

$\mu_\mathrm{r} = 100$ $\mu_0\sigma = 100$

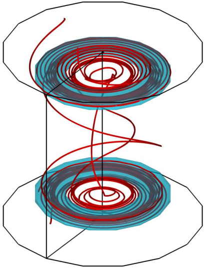

$\mu_\mathrm{r} = 100$

$B_\varphi \gg B_r, B_z$

toroidal field dominates

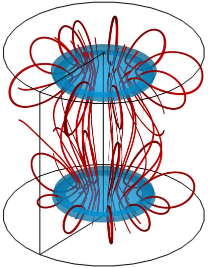

$\mu_0\sigma = 100$

$B_\varphi \ll B_r, B_z$

poloidal field dominates

Structure of field geometry essentially determined by material properties